Δελτίο της Ελληνικής Γεωλογικής Εταιρίας, τόμος L, σελ. 1485-1494
Πρακτικά 14ου Διεθνούς Συνεδρίου, Θεσσαλονίκη, Μάιος 2016

Bulletin of the Geological Society of Greece, vol. L, p. 1485-1494
Proceedings of the 14th International Congress, Thessaloniki, May 2016

STRESS EVOLUTION ONTO MAJOR FAULTS IN MYGDONIA BASIN

Gkarlaouni G.C.[1], Papadimitriou E.E.[1] and Kilias A.A.[2]

[1]*Aristotle University of Thessaloniki, Department of Geophysics, 54124, Thessaloniki, Greece, hara.gkarlaouni@geo.auth.gr, ritsa@geo.auth.gr*

[2]*Aristotle University of Thessaloniki, Department of Geology, 54124, Thessaloniki, Greece, kilias@geo.auth.gr*

Abstract

Stress transfer due to the coseismic slip of strong earthquakes, along with fault population characteristics, constitutes one of the most determinative factors for evaluating the occurrence of future events. The stress Coulomb (ΔCFF) evolutionary model in Mygdonia basin (N.Greece) is based on the coseismic changes of strong earthquakes (M≥6.0) from 1677 until 1978 and the tectonic loading expressed with slip rates along major faults. In the view of stress transfer mechanisms, ΔCFF is also calculated onto fault planes, along with the segmented fault zone from Thessaloniki to Gerakarou and N.Apollonia (TG-NAp FZ). Normal fault segments bound the basin from the south and currently compose the most active neotectonic zone. The association of the spatial distribution of seismicity (2000-2014) with the stress enhanced areas is also investigated. Results demonstrate that the earthquake locations are strongly influenced by the stress transfer from past strong earthquakes and their focal properties. Since the stress build-up occurs fast, results are discussed in terms of hazard assessment by defining potential locations for future events.
Keywords: *Coulomb stress, onto fault stress, Mygdonia basin.*

Περίληψη

Οι μηχανισμοί μεταφοράς τάσεων εξαιτίας των ισχυρών σεισμών, σε συνδυασμό με τα ιδιαίτερα χαρακτηριστικά των πληθυσμών ρηγμάτων επηρεάζουν τις διαδικασίες της σεισμογένεσης μελλοντικών σεισμών. Το εξελικτικό πεδίο των τάσων Coulomb υπολογίστηκε για την περιοχή της Μυγδονίας λεκάνης (Β. Ελλάδα) λαμβάνοντας υπόψιν τις μεταβολές της τάσης λόγω των ισχυρών σεισμών (M≥6.0) από το 1677 μέχρι και το 1978 αλλά και τη συσσωρευμένη παραμόρφωση η οποία εκφράζεται μέσω του ρυθμού ολίσθησης των ενεργών ρηγμάτων. Το εξελικτικό πεδίο των τάσεων υπολογίστηκε και κατά μήκος της ενεργούς ρηξιγενούς ζώνης Θεσσαλονίκης-Γερακαρούς-Ν.Απολλωνίας (TG-NAp FZ). Η ζώνη αυτή οριοθετεί τη λεκάνη από το Νότο και αποτελείται από διαδοχικά τεμάχη ρηγμάτων. Αναδεικνύεται η σχέση των περιοχών με θετικές μεταβολές Coulomb με την επικεντρική κατανομή των ισχυρών σεισμών αλλά και της μικροσεισμικότητας. Δεδομένου ότι στην περιοχή οι τάσεις ανακτώνται σημαντικά, ορίζονται οι πιθανές περιοχές για μελλοντικούς σεισμούς.
Λέξεις κλειδιά: *Εξελιξικτικό μοντέλο Coulomb, Μυγδονία λεκάνη.*

1. Introduction

The role of stress transfer in hazard assessment has been widely documented even for small magnitude earthquakes, since it combines the result generated from the long-term tectonic loading and the sudden redistribution of stresses due to earthquake coseismic dislocations (King, 1994; Toda *et al.*, 1998). The association between strong and recent seismicity in terms of stress distribution in Mygdonia basin (N. Greece) and stress interaction among faults are the main objectives of this study. Mygdonia basin was selected because it comprises a well-defined fault population and precisely located recent seismicity (Gkarlaouni *et al.*, 2014). The methodology incorporates coseismic stress changes on faults which are approximated with rupture models and fault slip rates derived from geodetic measurements. The evolutionary Coulomb stress field was calculated and shown both in three dimensions and across the planes of the dominant rupture zones, in order to measure the degree of interaction between adjacent faults. An additional objective was to define the way that stress is accumulated and distributed along faults depending on the variations of the fault plane solutions and its direct impact on faults interactive behavior.

2. Study Area

2.1. Seismotectonic Setting

Mygdonia is frequently struck by devastating earthquakes although currently is in a seismic quiescence. The recent seismicity pattern is characterised by a small number of moderate events (4.0≤M≤5.8) localised along seismogenic zones. Strong earthquakes (M≥6.0) are documented since 677AD (Papazachos and Papazachou, 2003) with their epicentres mostly distributed between the southern and the northern boundaries (Figure 1). It represents a rotated basin surrounded by mountainous blocks, being the most active region of N.Greece. The fault population comprises a synthesis of E-W, NW-SE and NE-SW rupture zones, an inherited fault network from the previous deformation episodes (Pavlides and Kilias, 1987; Chatzipetros and Pavlides, 1998; Tranos *et al.*, 2003 and references within, Zervopoulou and Pavlides, 2005). There is evidence that strong earthquakes are associated with the E-W normal faults which dominate, however, small NE-SW faults are also associated with the current seismic activity.

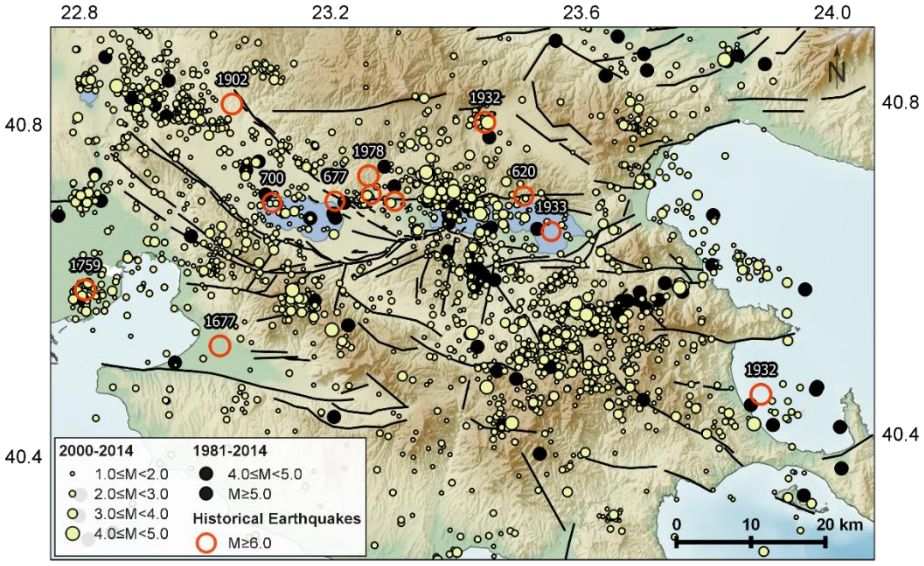

Figure 1 - The seismotectonic properties of Mygdonia basin and its surrounding area.

2.2. Fault Segmentation and Slip Rates

Continuous extension in the study area is controlled by the westward extrusion of the Aegean microplate, accommodated southern than the North Aegean Trough (NAT), the subduction and the rolling back of the Mediterranean slab. The study area, located northern than NAT, belongs to the back-arc region, characterized by extension in lower rate of the order of 1mm/yr as geodetic measurements reveal (Kotzev *et al*., 2006). After the occurrence of the strong 1978 earthquakes in Stivos, Martinod *et al*. (1997) measured an extension equal to 5.7mm/yr , at the southern margin of Mygdonia graben within 20 years, interpreted as a combined effect between post seismic relaxation and continuous aseismic extension. Tranos *et al*. (2003) proposed an even smaller slip rate equal to 0.4mm/yr based on geological data. Evaluating the geodetic and geological measurements a slip of 1mm/year was attributed to all the well defined regional faults (Figure 2). Estimation of the strain accumulation on the most important zones requires their classification into separate segments, according to the seismotectonic information on their properties. Details about the fault segments like, the fault length (L), the mean coordinates (λ and φ), the azimuth (ζ), the dip (δ), the horizontal (u_{SS}) and along dip (u_{DS}) components of the long-term slip rate of faults are provided for all 28 distinct fault segments (S_1-S_{28}, Table 1).

Table 1 - Fault segmentation and long term slip rates on major faults.

S	Fault Name	L (km)	Mean coordinates		ζ (°)	δ (°)	Slip Rate	
			(λ°E)	(φ°N)			u_{SS} (m/y)	u_{DS} (m/y)
S_1	Lag1	8.8	22.94414	40.75666	310	45	0.0	0.001
S_2	Lag2	10.0	23.02936	40.69975	310	45	0.0	0.001
S_3	Lag3	11.6	23.14092	40.64348	300	45	0.0	0.001
S_4	PP	12.9	22.89163	40.73381	310	45	0.0	0.001
S_5	PAs	12.8	23.00976	40.65710	310	45	0.0	0.001
S_6	AsCh	11.3	23.13911	40.61727	278	46	0.0	0.001
S_7	Ger	14.6	23.28629	40.64321	278	46	0.0	0.001
S_8	NAp1	11.3	23.44274	40.64267	270	46	0.0	0.001
S_9	NAp2	14.0	23.58600	40.62324	260	46	0.0	0.001
S_{10}	Anth1	16.7	23.06817	40.48069	278	53	0.0	0.001
S_{11}	Anth2	19.5	22.85708	40.51393	278	53	0.0	0.001
S_{12}	Zagl	14.4	23.28954	40.56161	310	45	0.0	0.001
S_{13}	Ass1	18.5	23.10439	40.78157	130	53	0.0	0.001
S_{14}	Ass2	6.2	23.21406	40.70125	110	53	0.0	0.001
S_{15}	Str	17.8	23.92095	40.51890	90	53	0.0	0.001
S_{16}	Sch	20.0	23.25890	40.81749	90	53	0.0	0.001
S_{17}	Mv	9.7	23.47184	40.81371	90	53	0.0	0.001
S_{18}	Arn	9.0	23.67564	40.50984	230	45	0.0	0.001
S_{19}	Ier	16.0	23.76382	40.41040	130	45	0.0	0.001
S_{20}	Sig	6.8	23.74786	40.35178	130	45	0.0	0.001
S_{21}	Anth3	16.0	23.22012	40.43156	278	53	0.0	0.001
S_{22}	N	15.0	23.03187	40.59478	45	80	0.0	0.001
S_{23}	N	8.5	23.13387	40.59596	45	80	0.0	0.001
S_{24}	N	9.0	23.08580	40.62488	45	80	0.0	0.001
S_{25}	V1	11.3	23.47037	40.69835	90	45	0.0	0.001
S_{26}	V2	8.2	23.56338	40.68897	90	45	0.0	0.001
S_{27}	Ger	9.8	23.36250	40.51545	130	45	0.0	0.001
S_{28}	Str	16.0	23.71427	0.53817	110	53	0.0	0.001

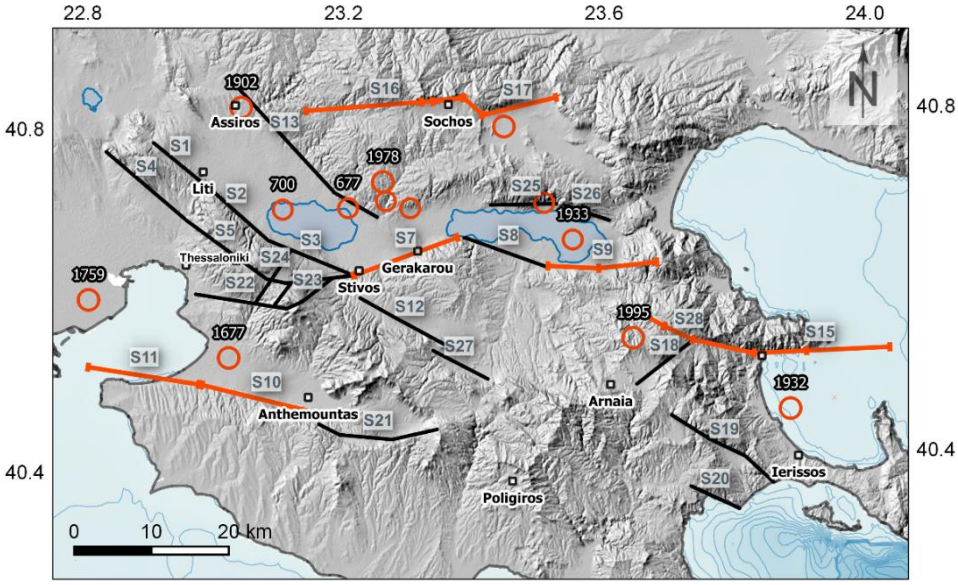

Figure 2 - Fault segmentation of the study area: Lagina- Agios Vasileios (LAV, S1-S2), Pilea-Peristera (PP, S3-S4), Asvestochori-Chortiatis (AsCh, S23). Gerakarou-Nea Apollonia (Ger, NAp1, NAp2, S7-S9) fault zone, comprised of three segments (S7-S9), Anthemountas - Skepasto fault (AnF, S10-S11-S21), Stratoni Fault (StF, S28-S15), Gomati-Ierissos (IF, S19-S20). To the north, Sochos (SF, S16) and Mavrouda fault (MvF, S17), Arnea Fault (ArF, S18), Zagliveri fault (ZF, S12) and Geroplatanos fault (GF, S27) which show a geomorphological continuation of the LAV fault to the east.

3. Methodology and Rupture Models

3.1. Methodology

The methodology used for the calculation of Coulomb stress changes is proposed by Deng and Sykes (1997) and is based on the elastic rebound theory, according to which, the stress released in an earthquake pre-exists before the event. For the estimation of interseismic strain on the major fault zones attributed to aseismic motions the so-called "virtual dislocation" model is adopted. This concept assumes that the accumulated stress can be determined by assuming that the fault slips backwards powered by the tectonic loading. The suggested model refers to a planar orthogonal fault surface, Σ, with finite dimensions, embedded in an elastic half space (Okada, 1992) whose displacement is given by Eq.1 (Steketee, 1958). Elastic stress, derives from strain, S_{ij}, using Hooke's law, for an isotropic medium**.**

Equation 1 - The equation for the stress tensor

$$s_{ij} = \frac{2\mu\nu}{1-2\nu}\delta_{ij}e_{kk} + 2\mu e_{ij}$$

where μ is the shear modulus, ν is the Poisson's ratio and δ_{ij} is the Kronecker delta. Earth is treated as an elastic structure, where postseismic deformation is negligible. Modulus and Poisson's ratio are fixed as 33GPa and 0.25, respectively. The Coulomb fracture criterion examines the conditions under which failure occurs on brittle rocks (Scholz, 2002). According to this criterion, earthquakes

occur when Coulomb stress exceeds the strength of the rock. Changes in Coulomb failure function (ΔCFF) depend on the change in shear Δτ, and normal stress, Δσ, respectively calculated by Eq.2.

Equation 2 - Change in Coulomb failure function (ΔCFF)

$$\Delta CFF = \Delta\tau + \mu'\Delta\sigma$$

where, μ' is the apparent coefficient of friction. Parameter μ' incorporates the effect of pore fluids and fault zone material properties and is given by μ'=μ·(1–B). B is the Skempton's coefficient, and varies between 0 and 1. The involvement of μ' into the change of pore pressure has been widely investigated and oftentimes is treated as a material constant or a time dependent parameter varying before and after an event. It has been shown that μ' low values are related to weak fault zones accompanied with well-developed gouge often saturated with fluids (Stein, 1999). Different μ' values have been tested not opposing dramatic modifications in the overall stress pattern. Finally μ' in this study is taken equal to 0.4.

3.2. Rupture Models

Fault sources associated with the strong earthquakes are geometrically approximated with rectangular sources embedded into the brittle crust. Fault length, width, strike, dip and rake are the main parameters describing the rupture zones and further used for stress calculation. These parameters are inferred from the interpretation of the available geological or seismological information and in the absence of these data, appropriate empirical relationships have been used (Papazachos *et al*., 2004). The average displacement and its components are based on the seismic moment and on observations upon the distribution of earthquake foci. Model source parameters are displayed in Table 2, where magnitudes with asterisks are estimated from historical macroseismic information (Papazachos and Papazachou, 2002).

Table 2 - Model sources for strong earthquakes (M≥6.0) for the period 1677-2014.

Time	Epicenter		Code	M_W	M_o (10^{25})	L (km)	W (km)	Fault Plane Solution			Average displacement		Ref
Year	(φ◦)	(λ◦)						ζ (◦)	δ (◦)	λ (◦)	u_{SS} (m)	u_{DS} (m)	
1677	40.50	23.00	AnF	6.2*	2.04	17	15	278	53	-93	-0.023	0.439	1, 2
1759	40.60	22.80	AnF	6.3*	2.88	19	15	278	53	-93	-0.027	0.519	1, 2
1902	40.80	23.04	SF	6.5*	8.13	25	15	90	53	-93	-0.037	0.719	1, 2
1932	40.40	23.76	IerF	7.0*	32.4	25	15	93	53	-93	-0.102	1.957	1, 2
1932	40.79	23.44	SF	6.2*	2.04	17	15	90	53	-93	-0.023	0.439	1, 2, 3
1933	40.65	23.54	NAF	6.3*	2.88	19	16	278	46	-70	0.177	0.488	1, 2,3
1978	40.73	23.25	TGF	6.5	5.20	21	16	278	46	-70	0.154	0.423	4

[1]Papazachos and Papazachou (2002); [2]Hanks and Kanamori (1979), [3]Paradeisopoulou *et al.* (accepted); [4] Soufleris and Stewart (1981)

4. Stress Field in Mygdonia

4.1. Evolutionary Stress Field

The evolutionary stress field results from the accumulation of the successive stress changes due to the co-seismic displacements described in Table 2, along with the constant impact on major faults, modelled in Table 1. Results are shown in successive figures (Figure 3). Before the occurrence of the 1678 Vassilika event, *ΔCFF* changes are considered to be zero, in the broader area. Any information on earthquakes before 1678 is disregarded, since going back in time, the uncertainties in earthquake location and magnitude are increased. Moreover, no strong earthquakes are

documented for more than 10 centuries, before. Successive chronological intervals are considered, just before the occurrence of the consecutive strong event. In each case, the stress field is computed according to the fault plane solution of the following event (the responsible fault is depicted with white color). Dark blue regions correspond to negative changes in stress and infer a decreased likelihood of a fault rupture (stress shadows). Yellow to red regions represent positive *ΔCFF* and an increased likelihood of a fault rupture (bright zones).

The initial stress changes are caused by the co-seismic slip of the 1677 event in AnF (Figure 3a). The stress pattern corresponds to a typical E-W normal fault, which imposes a stress enhancement to the east (central Chalkidiki) and the west (Thermaikos gulf). In particular, the along fault prolongation of AnF fault to the west is covered with a bright zone of positive stress changes (Figure 3b), where 82 years after, the next strong earthquake of the same magnitude order occurs (1759 Thessaloniki earthquake, M_w6.5). The co-seismic changes after the aforementioned events along with the tectonic loading, reinforce the prevalence of positive stresses to the central part of Mygdonia. According to historical information the following earthquake occurred near the western termination of the south dipping Soch. fault, in 1902 (Figure 3c). The stress field calculated for the south dipping normal Str. F, before the 1932 earthquake of Ierissos is presented in Figure 3d, where extensive bright zones are distributed over the central and the eastern parts of the study area. The 1902 event triggered the occurrence of the next two smaller earthquakes in 1932 (some months after Ierissos strong event) as well as in 1933, whose epicentral accuracy is on debate. These events were strongly advanced because of stress transfer from the severe Ierissos earthquake, since they occurred within the eastern positive lobe of the stress changes pattern. The 1932 earthquake is probably attributed to the termination of Soch. fault and its coalescence with Mavrouda segment (Mav.F.) to the east. It is shown that before the occurrence of this event there is a bright zone restricted between the shadow zones caused by the 1932 Ierissos and previous earthquakes (Figure 3e). The stress field calculated for the northdipping normal fault responsible for the 1932 Sochos event is shown in Figure 3f. 46 years later the most recent recorded strong shock occurred in the central part of Mygdonia graben where extensive stress enhanced areas exist (Figure 3g). Finally the current distribution of stresses is calculated for a northdipping normal fault typical for Mygdonia area (Figure 2h). Stresses are significant in the central part of Mygdonia, while the area of Anth. fault and the western segment of Soch. fault remain in stress shadow, prohibiting earthquake triggering in these areas.

4.2. Onto fault ΔCFF

The second objective of the study is the quantification of the accumulated coseismic stress changes of the strong earthquakes onto plane of the major rupture zone of the Thessaloniki - Gerakarou - N.Apollonia fault zone (TG-Nap FZ). This study is motivated from the fact that faults interact through their stress field even if they are not mechanically connected. From west to east the fault planes are the PPF (S_5), AchF (S_6), St.F (S_7), NAp1F (S_8) and NAp2 (S_9), which are considered rectangles embedded into the brittle crust. The interaction between the fault segments of the same rupture zone, even when earthquakes occur on adjacent faults of the same fault population, play an important role in fault mechanics. Therefore, the amount of stress enhancement by earthquake occurrence in parallel, antithetic or adjacent faults is approximated. The stress changes due to co-seismic slip of the strong earthquakes ($M \geq 6.0$) are resolved onto the planes of the five fault segments. The accumulated stress changes are calculated according to the faulting type of the next strong earthquake in the data set and consequently the associated fault segment. Stress changes are calculated for the depth of 1.0-20km within the brittle crust and results are shown in the sub plots of Fig. 4. The cumulative effect of the two 1678 and 1759 events associated with east and west segments of AnF, are shown onto the five fault planes. The S7 and S8 segments are covered by high negative values of *ΔCFF* (1st row, Fig. 4). The occurrence of the 1902 event on the antithetic Soch.F imposes considerable stress disturbances, producing positive *ΔCFF* (stress enhancement) from 10 to 20km in S_7, which is the central part of the rupture zone (2nd row, Fig. **4**). After the strong Ierissos shock there is a stress increase onto the eastern part of the fault zone S_8 - S_9 (3rd row, Fig. 4), whereas there is no change at the central and the western part.

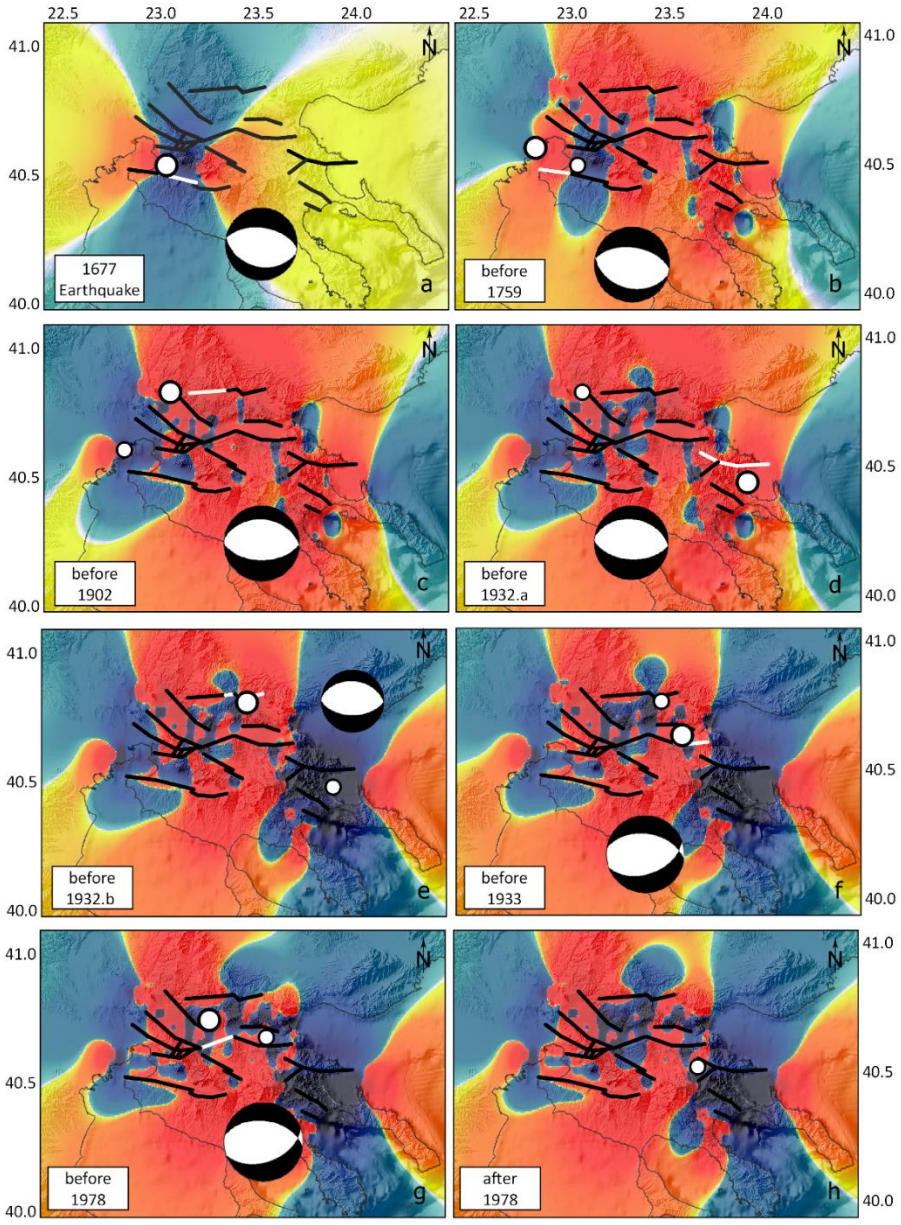

Figure 3 - Evolutionary stress field in Mygdonia a) coseismic stress changes associated with the 1677 Vassilika event, b) stress changes before the 1759 Anthemountas earthquake, c) stress field before the 1902 Assiros event, d) stress Coulomb changes before the 1932 Ierissos earthquake, e) stress changes before the 1932 Sochos earthquake, f) stress field before 1933 Volvi, g) stress field before the 1978 Stivos triplet, h) the current stress state, the epicentre of the strongest recent earthquake is shown (1995, M_w5.8). Coulomb stress changes are calculated for the fault plane solutions shown in each case and for 8km at depth.

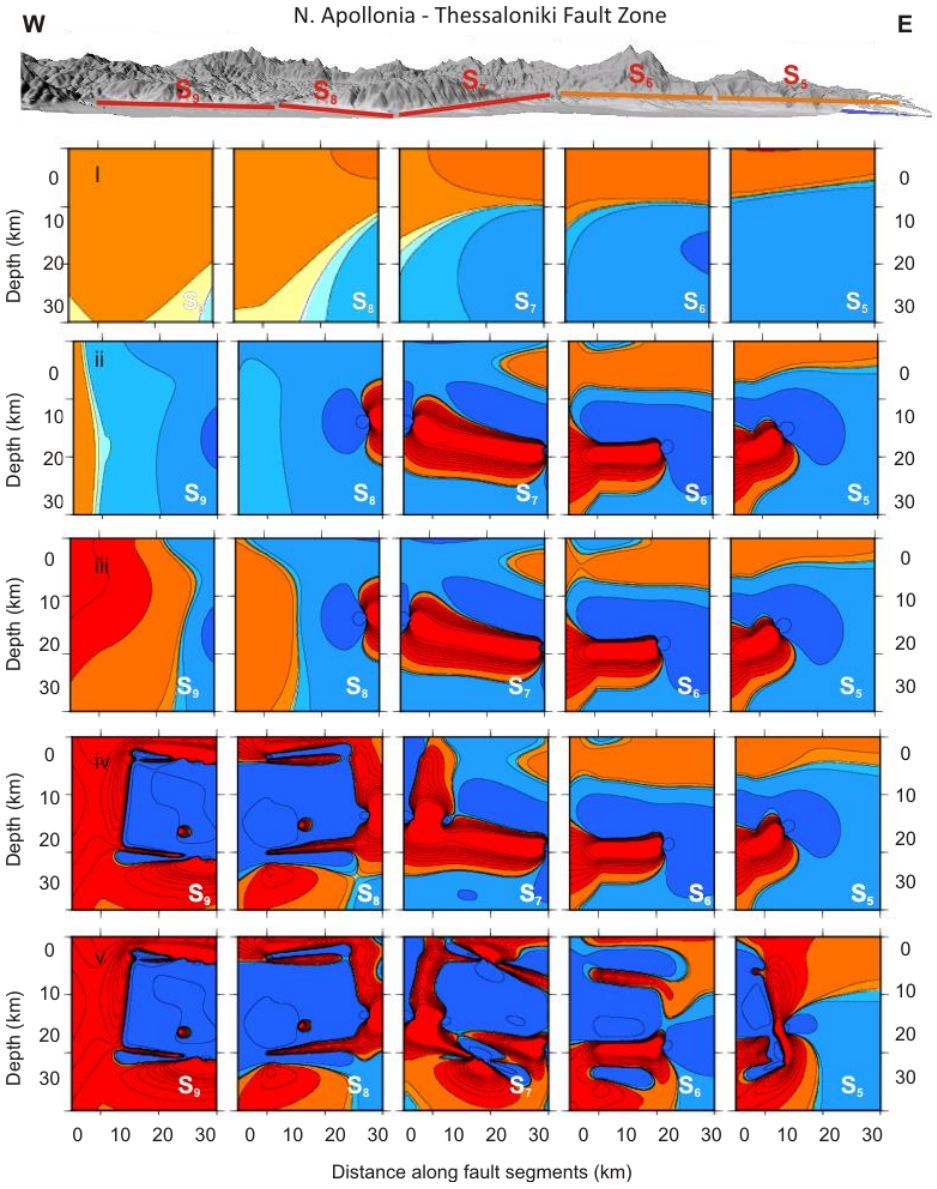

Figure 4 - At the top, the hanging wall relief of TG-NAp rupture zone with view from the North. View from the North Successive snapshots of Coulomb stress evolution onto the segments of TG-NAp FZ (S5-S9), i) The 1st row shows the coseismic stress changes after the 1677 and 1759 earthquakes along An.F, ii) the 2nd row presents the stress changes after 1902 Assiros event. iii) the 3rd row shows the effect of 1932 Ierissos earthquake, iv) the 4th row shows the stress changes after the 1932 Sochos and 1933 Volvi earthquakes, v) finally in the 5th row the stress field after the occurrence of the 1978 Stivos earthquake is calculated.

After some months Volvi and Sochos earthquake events occur and they created a shadow zone along NApF and GerF enforcing positive stress changes at the fault tips (4th row, Fig. 4). Finally, S7 became the causative source of the 1978 strong earthquake (5th row, Fig. 4) after which an extensive shadow zones is expanding along the entire rupture zone. An accumulation of increased stress values is mostly accommodated at the eastern end of the rupture zone.

4.3. Discussion - Conclusions

The double objective of this work, is the exploitation of the historical seismicity and their impact on the stress field and the constant loading on faults obtained from geodetic data. Stress changes due to the coseismic slip of strong earthquakes that occurred in the study area from 1677 until now are considered. *ΔCFF* changes are shown in map views and onto plane of the five major fault segments which comprise the southern boundary of Mygdonia basin. Recent seismicity in the time interval 2000 until 2014 with relocated focal coordinates (Gkarlaouni *et al*., 2015) show that most of the earthquakes are concentrated in locations with increased stress values (Fig. 5) for a stress field oriented for a typical north dipping normal fault.. A strong association between bright zones and strong or minor earthquakes occurrence is a characteristic feature. Current stress enhanced areas with an increased likelihood for earthquake occurrence are identified at the western part of Mygdonia and central Chalkidiki. The onto fault stress changes along the north dipping rupture zone which bounds Mygdonia graben from the south, showed that exist considerable interrelations exist in adjacent faults.

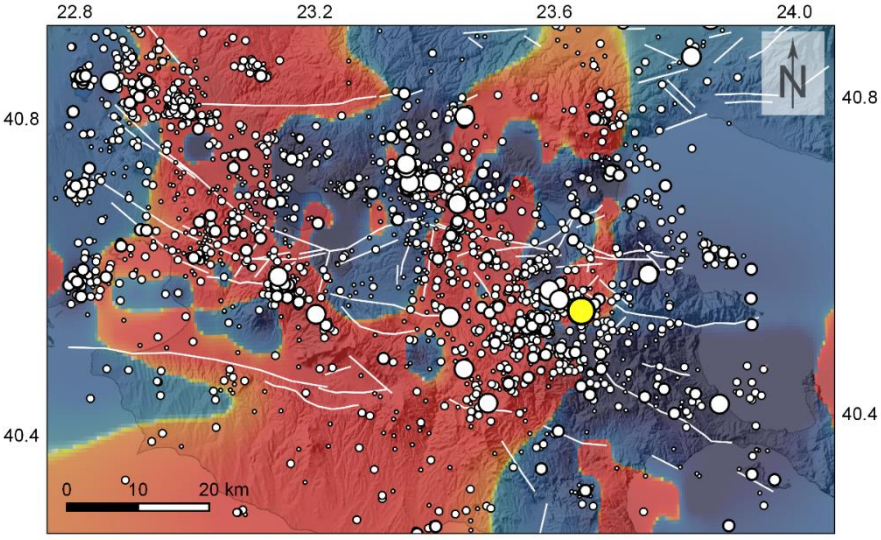

Figure 5 - The current stress state after the last 1978 earthquake along with the relocated seismicity for 2000 - 2014, for a typical north dipping fault (strike:278°, dip:45°, rake:78°) The epicentre in yellow represents the 1995 event, located in Arnea.

5. Acknowledgments

The authors would like to thank the editor and the two anonymous reviewers for their valuable contribution to the improvement of the paper. This research was co–financed by the European Union (European Social Fund–ESF) and Greek national funds through the Operational Program "Education and Lifelong Learning" of the National Strategic Reference Framework (NSRF) – Research Funding Program: Heracleitus II Investing in knowledge society through the European Social Fund. Stress tensors were calculated with Dis3D (Erikson L., 1986). Plots were made with QGIS (http://qgis.osgeo.org). Department of Geophysics, AUTh, Contribution number 853.

6. References

Chatzipetros, A. and Pavlides, S., 1998. A Quantitative Morphotectonic Approach to the study of active faults, Mygdonia basin, Northern Greece, *Bul.Geol.Soc*.

Deng, J. and Sykes, L., 1997. Evolution of the stress field in southern California and triggering of moderate–size earthquakes: A 200-year perspective, *J. Geophys. Res*., 102, 9859-9886.

Erikson, L., 1986. User's manual for DIS3D: a three-dinensional dislocation program with applications to faulting in the Earth, *MSc Thesis*, Standford University, 67.

Goldsworthy, M. and Jackson, J., 2001. Migration of activity within normal fault systems: examples from the Quaternary of mainland Greece, *J. Struct. Geol.,* 23(2), 489-506.

Gkarlaouni, C., Papadimitriou, E., Karakostas, V., Kilias, A. and Lasocki, S., 2015. Fault population recognition through microseismicity in Mygdonia region (northern Greece), *Bollettino di Geofisica Teorica ed Applicata*, 56 (3) 367-382, doi: 10.4430/bgta0153.

Hanks, T. and Kanamori, H., 1979. A moment magnitude scale, *J.Geophys.Res.*, 34, 2348-2350.

King, G., Stein, R. and Lin, J., 1994. Static stress changes and the triggering of earthquakes, *Bull. Seismol. Soc. Am.*, 84, 935-953.

Kissel, C., Laj, C. and Muller, C., 1985. Tertiary geodynamical evolution of northwestern Greece: paleomagnetic results, *Earth Plant. Sci. Lett.*, 72, 190-204.

Kotzev, V., Nakov, R., Georgiev, T., Burchfiel, B. and King, R., 2001. Crustal motion and strain accumulation in western Bulgaria, *Tectonophysics*, 413, 189-200.

Martinod, J., Hatzfeld, D., Savvaidis, P. and Katsambalos, K., 1997. Rapid N-S extension in the Mygdonian graben (Northern Greece) deduced from repeated geodetic surveys, *Geophys. Res. Letters*, 24(24), 3293-3296.

Okada, Y., 1992. Internal deformation due to shear and tensile faults in a half space, *Bull. Seism. Soc. Am.*, 82, 1018-1040.

Papazachos, B. and Papazachou, C., 2003. *The earthquakes of Greece*, Ziti Publication, 304, Thessaloniki.

Papazachos, B.C., Scordilis, E.M., Panagiotopoulos, D.G., Papazachos, C.B. and Karakaisis, G F., 2004. Global relations between seismic fault parameters and moment magnitude of earthquakes, *Bull. Geol. Soc. Greece*, 36, 1482-1489.

Paradisopoulou, P., Papadimitriou, E. and Mirek, J., (*accepted*). Signifficant earthquakes near the city of Thessaloniki (N.Greece) and probability distribution on faults, *Bull. Geol. Soc. Greece*.

Pavlides, S. and Kilias, A., 1987. Neotectonic and active faults along the Serbomacedonian zone (SE Chalkidiki, northern Greece), *Ann.Tectonicae*, 1, 97-104.

Scholz, C.H., 2002. *The mechanics of earthquakes and faulting*, Cambridge University press, Cambridge, 439.

Soufleris, C. and Steward, G., 1981. A source study of the Thessaloniki (northern Greece) 1978 earthquake sequence, *Geophys. J. R. Astron. Soc.*, 67, 343-358.

Stein, R., 1999. The role of stress transfer in earthquake occurrence, *Nature*, 402, 605-609.

Steketee, J., 1958. On Voltera's dislocations in a semi-infinite elastic medium, *Can J Phys*, 36, 192-205.

Toda, S., Stein, R., Reasenberg, A., Dieterich, H. and Yoshida, A., 1998. Stress transferred by the 1995 Mw=6.9 Kobe, Japan, shock: Effect on aftershocks and future earthquake probabilities, *J. Geophys. Res.*, 103, 24.543-24.565.

Tranos, M., Papadimitriou, E. and Kilias, A., 2003. Thessaloniki-Gerakarou fault zone (TGFZ): the western extension of the 1978 Thessaloniki earthquake fault (northern Greece) and seismic hazard assessment, *J. Struct. Geol.*, 25, 2109-2123.

Zervopoulou, A. and Pavlides, S., 2005. Morphotectonic study of the broader area of Thessaloniki for the cartography of neotectonic faults, *Bull. Geol. Soc. Greece*, XXXVIII, 30-41.